



Published in final edited form as:

*Adv Exp Med Biol.* 2011 ; 701: 207–213. doi:10.1007/978-1-4419-7756-4\_28.

## Heterogeneity of Mitochondrial Redox State in Premalignant Pancreas in a PTEN Null Transgenic Mouse Model

**He N. Xu,**

Department of Radiology, School of Medicine, University of Pennsylvania, Philadelphia, PA, USA

**Shoko Nioka,**

Johnson Research Foundation, Department of Biochemistry and Biophysics, School of Medicine, University of Pennsylvania, Philadelphia, PA, USA

**Britton Chance,** and

Johnson Research Foundation, Department of Biochemistry and Biophysics, School of Medicine, University of Pennsylvania, Philadelphia, PA, USA

**Lin Z. Li**

Department of Radiology, School of Medicine, University of Pennsylvania, Philadelphia, PA, USA

### Abstract

Pancreas-specific deletion of PTEN in mice revealed progressive premalignant lesions such as ductal metaplasia with infrequent malignant transformation. In this study, we aimed at evaluating the mitochondrial redox state of the metaplastic pancreas in a pancreas-specific PTEN null transgenic mouse model. The two intrinsic fluorophores, reduced nicotinamide adenine dinucleotide (NADH) and oxidized flavoproteins (Fp) such as flavin adenine dinucleotide (FAD), in the respiratory chain in mitochondria are sensitive indicators of mitochondrial redox states and have been applied to the studies of mitochondrial function with energy-linked processes. The redox ratio, Fp/(Fp+NADH) provides a sensitive index of mitochondrial redox state. We have obtained optical images of the *in vivo* mitochondrial redox states of the snap-frozen pancreases from pancreas-specific PTEN null mice (Pdx1-Cre;PTEN<sup>lox/lox</sup>, N=3) and the controls (PTEN<sup>lox/lox</sup>, N=3) using the redox scanner at low temperature. The results showed high spatial heterogeneity of mitochondrial redox state in the mutated pancreases with hot spots of much higher Fp redox ratios whereas the normal ones, were relatively homogenous. The cystic dilation regions in the metaplastic pancreases showed little to no NADH or Fp signal. Histological analysis confirmed no cells existed in these regions. It is the first time that the *in vivo* mitochondrial redox states of the metaplastic mouse pancreas were optically imaged. Our previous results on human melanoma and breast cancer mouse xenografts have shown that mitochondrial redox state quantitatively correlates with cancer metastatic potential. The more oxidative mitochondrial redox state (higher Fp redox ratio) corresponded to the higher metastatic potential of the tumors. As mitochondrial redox state imbalance is associated with abnormal mitochondrial function, and redox state mediates the generation of reactive oxygen species and many signal transduction pathways, this research may provide insights for studying basic biology and developing early diagnostic imaging biomarkers for pancreatic cancer.

## 28.1 Introduction

Early detection of pancreatic cancer demands reproducible imaging biomarkers. Pancreas-specific deletion of PTEN in mouse revealed progressive premalignant lesions such as ductal metaplasia with infrequent malignant transformation [1]. PTEN is a tumor suppressor gene inhibiting the activity of PI3K/Akt signaling pathway, which plays a key role in cancer progression. This premalignant pancreatic cancer model provides an excellent tool for searching for biomarkers in early pancreatic cancer detection. In mitochondria, the two intrinsic fluorophores, reduced nicotinamide adenine dinucleotide (NADH) and oxidized flavoproteins (Fp) such as flavin adenine dinucleotide (FAD), in the respiratory chain are sensitive indicators of mitochondrial redox states and have been applied to the studies of mitochondrial function with energy-linked processes. The redox ratio, Fp/(Fp+NADH) provides a sensitive index of mitochondrial redox [2–6].

Previously, by using the low-temperature redox scanning technique [6–9] we discovered that *in vivo* mitochondrial redox state is a sensitive marker distinguishing between normal tissue and human melanoma xenografted in mice [10] and differentiating tumor aggressiveness among five human melanoma tumor lines spanning a wide range of metastatic potential in mouse xenografts [11]. In the present investigation, we report the preliminary results of quantitative mitochondrial redox imaging of mouse pancreases using the pancreas-specific PTEN knockout mice as the model system. The possible link between the premalignant lesions in the pancreas and the *in vivo* mitochondrial redox state, provides insights for basic biology studies and may aid the development of early diagnostic imaging biomarkers for pancreatic cancer.

## 28.2 Methods

Three PTEN null mice (Pdx-1-Cre;PTEN<sup>lox/lox</sup>) and three control mice (PTEN<sup>lox/lox</sup>) were prepared in the Stanger laboratory [1]. All mice were about 8 months old. The pancreases of the anesthetized mice were quickly resected and dipped into liquid nitrogen within 2 seconds after removal. The samples for redox scan were prepared as previously described [12, 13]. Briefly, a snap-frozen pancreas was carefully placed into the chilled mounting medium composed of ethanol-glycerol-water (10:30:60) contained in a plastic screw closure of 24 mm diameter. Frozen reference standards (one NADH and one Fp with known concentrations) were quickly mounted adjacent to the tissue. The screw closure containing the tissue and reference standards was then maintained in liquid nitrogen awaiting redox scanning.

The above prepared samples were redox-imaged under liquid nitrogen temperature using the redox scanner [6–9]. Briefly, the sample surface was first milled flat under liquid nitrogen by the grinder equipped with the scanner for redox scanning. A bifurcated fiberoptic probe driven by a stepper motor transmits the excitation photons from a mercury lamp and collects the emission photons from samples. The Fp excitation and emission filters are  $430 \pm 25$  nm and  $525 \pm 32$  nm, respectively; and those of NADH are  $360 \pm 26$  nm and  $430 \pm 25$  nm, respectively. The emission signals were transmitted to the photomultiplier tube and further processed by a personal computer to construct the NADH and Fp fluorescence images. The

scanning matrix was  $128 \times 128$  with a step size of  $100 \mu\text{m}$ . Multiple sections at different milling depths spacing  $100\text{--}400 \mu\text{m}$  were scanned for each pancreas (9 and 14 sections from the control group and the PTEN null group, respectively).

The acquired raw data were analyzed using MatLab<sup>®</sup> software to generate NADH and Fp and concentration-based Fp redox ratio ( $\text{Fp}/(\text{Fp}+\text{NADH})$ ) images. The inner area of each reference tube section was selected as the region of interest (ROI) for reference standards. The NADH signal from the Fp standard serves as the background signal for NADH channel and vice versa. The mean value of the signal intensities from each standard's image was computed with background signal subtraction. For tissue samples, ROIs were carefully drawn along the pancreas tissue rim. The NADH and Fp nominal concentrations in the tissue samples were obtained by comparing the fluorescence from tissue with that from the reference standards. Pixels having signals within 3-fold standard variations of the background signals were excluded from the analysis.

The mean value of Fp redox ratio, the standard deviation (SD) of the Fp redox ratio, the nominal concentrations of NADH and Fp, and the SD of these concentrations were obtained for the tissue ROI for each section subjected to redox scan, and then averaged across multiple sections for each pancreas to obtain the Fp redox ratio, SD of Fp redox ratio, NADH, Fp, SD of NADH, and SD of Fp for each individual pancreas. The group average values of these parameters from 3 pancreases in each group were also calculated to obtain the  $\bar{\text{Fp}}$  redox ratio,  $\bar{\text{SD}}$  of Fp redox ratio,  $\bar{\text{NADH}}$ ,  $\bar{\text{Fp}}$ ,  $\bar{\text{SD}}$  of NADH, and  $\bar{\text{SD}}$  of Fp. The statistical significance of the difference of these parameters between the two mouse groups was analyzed using unpaired t-tests.

### 28.3 Results

Figure 28.1 shows the typical images and their corresponding histograms of Fp redox ratio,  $\text{Fp}/(\text{Fp}+\text{NADH})$ , nominal concentration of Fp and NADH of two PTEN null pancreases in coronal and transversal section, respectively. Figure 28.2 shows the typical images and their corresponding histograms of Fp redox ratio,  $\text{Fp}/(\text{Fp}+\text{NADH})$ , nominal concentration of Fp and NADH of a normal pancreas. As clearly seen in Figure 28.1, the PTEN null pancreases are highly heterogeneous in their mitochondrial redox ratios. The cystic dilation area showed no fluorescent signal, indicating few or no cells in the regions. H&E staining of the adjacent sections revealed no cells in these regions (data not shown).

The average Fp redox ratio is 0.35 and 0.38 for the control and pre-malignant group, respectively (Table 28.1). The unpaired t-test shows that there is no significant difference in Fp redox ratio between the two groups. However, the average standard deviations of the Fp redox ratios are significantly different between the two groups ( $p=0.02$ ) with the control group having 0.06 and the pre-malignant group having 0.11, almost twice as large. The higher SD in the premalignant group is consistent with the wider peaks in the histograms of Fp redox ratio, indicating much higher heterogeneity in the distribution of mitochondrial redox states. Significant difference also exists in nominal concentration of NADH with the pre-malignant group having much lower NADH level. Additionally, a marginal difference ( $p=0.07$ ) is seen in nominal concentration of Fp with the premalignant group having lower

Fp level. The differences in the standard deviations of the fluorophore concentrations between the two groups are not significant.

## 28.4 Discussion

The redox images obtained in the present study revealed that significantly higher heterogeneity in the mitochondrial redox state was observed in PTEN knockout mice pancreases which were presumably undergoing metaplastic process. Studies suggested that the cellular basis of tumor progression was variability among subpopulations of tumor cells and such heterogeneity was associated with malignancy [14, 15]. Our previous studies on human melanoma and breast cancer mouse xenografts indicated that higher intratumor heterogeneity and higher Fp redox ratio were associated with more metastatic tumors as compared with indolent tumors [11, 16]. However, we did not observe a significant difference in the average value of Fp redox ratio between the PTEN null group and the control group. This may be partially explained by the fact that pancreas specific PTEN knockout only caused infrequent malignancy and premalignant lesions may only occupy a relatively small portion of the tissue distribution [1].

Therefore, the low average of Fp redox ratio of PTEN null pancreas may indicate that most of the cells were not yet cancerous, the “hot” spots of much higher Fp redox ratio might indicate premalignant transformation. The in-plane resolution in the redox images is 100  $\mu\text{m}$ , not capable of fully resolving the pancreas premalignant lesions involving the ductal formations (size  $\sim 200 \mu\text{m}$  or more). Ideally, if we could co-register our redox scanned section with the histology of the section, we may be able to tell if the hot spots correspond to premalignant lesions such as ductal metaplasia. However, such co-registration is practically difficult because the snap-frozen sample preparation has frozen the tissue at such a low temperature using liquid nitrogen, that it is not possible to slice the tissue, whereas raising the temperature for the tissue to melt distorts the tissue shape and histology. It may be worth developing tissue redox imaging *ex vivo* at a higher resolution so that morphological information on premalignant lesions might be obtained and correlated with mitochondrial redox state.

## 28.5 Conclusions

In this paper we reported our current progress in imaging the mitochondrial redox state in premalignant pancreas in the PTEN null transgenic mouse model. Compared to the control group, characteristically wider distribution of the mitochondrial redox states in the premalignant pancreases was delineated by the standard deviation of Fp redox ratio and by the wide peaks in the histograms of Fp redox ratio, indicating higher heterogeneity in their mitochondrial redox states. Our preliminary results suggested possible roles of mitochondrial redox states in pancreatic cancer transformation.

## Acknowledgments

This work was supported by the Susan G. Komen Foundation Grant KG081069 (PI: L.Z. Li) and National Institutes of Health-supported Research Resource Grant P41-RR002305 (PI: R. Reddy) and R01-CA155348 (PI: L.Z. Li). We would like to thank Dr. Ben Z. Stanger for providing the transgenic mice for this study and his valuable discussions.

We also appreciate Dr. Q.C. Yu for his valuable discussions on the histological analysis and Mr. Baohua Wu for his assistance, particularly in software development for data analysis.

## References

1. Stanger BZ, Stiles B, Lauwers GY, et al. PTEN constrains centroacinar cell expansion and malignant transformation in the pancreas. *Cancer Cell*. 2005; 8:185–95. [PubMed: 16169464]
2. Chance B, Williams GR. Method for the localization of sites for oxidative phosphorylation. *Nature*. 1955; 176:250–254. [PubMed: 13244669]
3. Chance B, Baltscheffsky H. Respiratory Enzymes in Oxidative Phosphorylation. *J Biol Chem*. 1958; 233:736–739. [PubMed: 13575447]
4. Chance B., Schoener, B. Fluorometric studies of flavin component of the respiratory chain in Flavins and Flavoproteins. Slater, EC., editor. Elsevier; Amsterdam: 1966. p. 510-519.
5. Chance B, Schoener B, Oshino R, et al. Oxidation-reduction ratio studies of mitochondria in freeze-trapped samples. NADH and flavoprotein fluorescence signals. *J Biol Chem*. 1979; 254:4764–4771. [PubMed: 220260]
6. Chance B. Optical Method. *Annu Rev Biophys Biophys Chem*. 1991; 20:1–28. [PubMed: 1867711]
7. Quistorff B, Haselgrove JC, Chance B. High spatial resolution readout of 3-D metabolic organ structure: An automated, low-temperature redox ratio-scanning instrument. *Anal Biochem*. 1985; 148:389–400. [PubMed: 4061818]
8. Gu Y, Qian Z, Chen J, et al. High-resolution three-dimensional scanning optical image system for intrinsic and extrinsic contrast agents in tissue. *Rev Sci Instrum*. 2002; 73:172–178.
9. Li LZ, Xu HN, Ranji M, et al. Mitochondrial redox imaging for cancer diagnostic and therapeutic studies. *Journal of Innovative Optical Health Sciences*. 2009; 2:325–341. [PubMed: 26015810]
10. Li LZ, Zhou R, Zhong T, et al. Predicting melanoma metastatic potential by optical and magnetic resonance imaging. *Adv Exp Med Biol*. 2007; 599:67–78. [PubMed: 17727249]
11. Li LZ, Zhou R, Xu HN, et al. Quantitative magnetic resonance and optical imaging biomarkers of melanoma metastatic potential. *Proc Natl Acad Sci U S A*. 2009; 106:6608–13. [PubMed: 19366661]
12. Xu, HN., Wu, B., Nioka, S., et al. Calibration of redox scanning for tissue samples. In: SPIE. , editor. *Proceedings of Biomedical Optics*. San Jose, CA: 2009 Jan 24. p. 7174-71742F.
13. Xu HN, Wu B, Nioka S, et al. Quantitative redox scanning of tissue samples using a calibration procedure. *Journal of Innovative Optical Health Sciences*. 2009; 2:375–385.
14. Heppner GH, Miller FR. The cellular basis of tumor progression. *Int Rev Cytol*. 1998; 177:1–56. [PubMed: 9378615]
15. Fidler IJ, Hart IR. Biological diversity in metastatic neoplasms: origins and implications. *Science*. 1982; 217:998–1003. [PubMed: 7112116]
16. Xu HN, Nioka S, Glickson JD, et al. Quantitative mitochondrial redox imaging of breast cancer metastatic potential. *Journal of Biomedical optics*. 2010; 15:036010. [PubMed: 20615012]

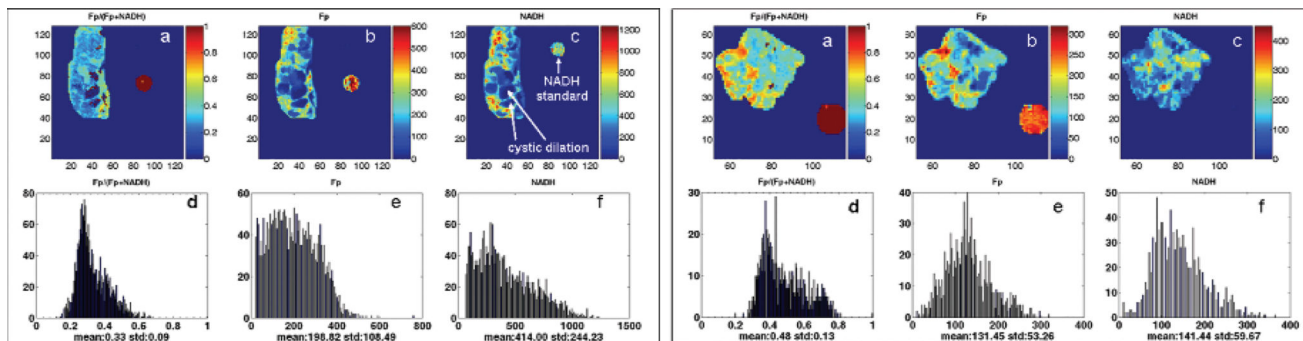


**Fig. 28.1.** Typical pseudo-color redox images (top row) and their corresponding histograms (bottom row) of PTEN null pancreases (left panel: coronal section, milling depth 1340  $\mu\text{m}$ ; right panel: transversal section, milling depth 100  $\mu\text{m}$ ). From left to right: Fp redox ratio (0–1); Fp nominal concentration ( $\mu\text{M}$ ); NADH nominal concentration ( $\mu\text{M}$ ). The color bar of Fp redox ratio image indicates the ratio range from 0–1. The color bars of Fp and NADH images indicate the nominal concentrations in  $\mu\text{M}$ . The x axes of the corresponding histograms represent the Fp or NADH concentration or redox ratio. The y axes represent the number of pixels in the tissue section having a specific value of redox ratio or fluorophore concentration. The round spots outside the tissue area are Fp or NADH reference standards; image matrix:  $128 \times 128$  (left panel) and  $64 \times 128$  (right panel); resolution: 100  $\mu\text{m}$ .

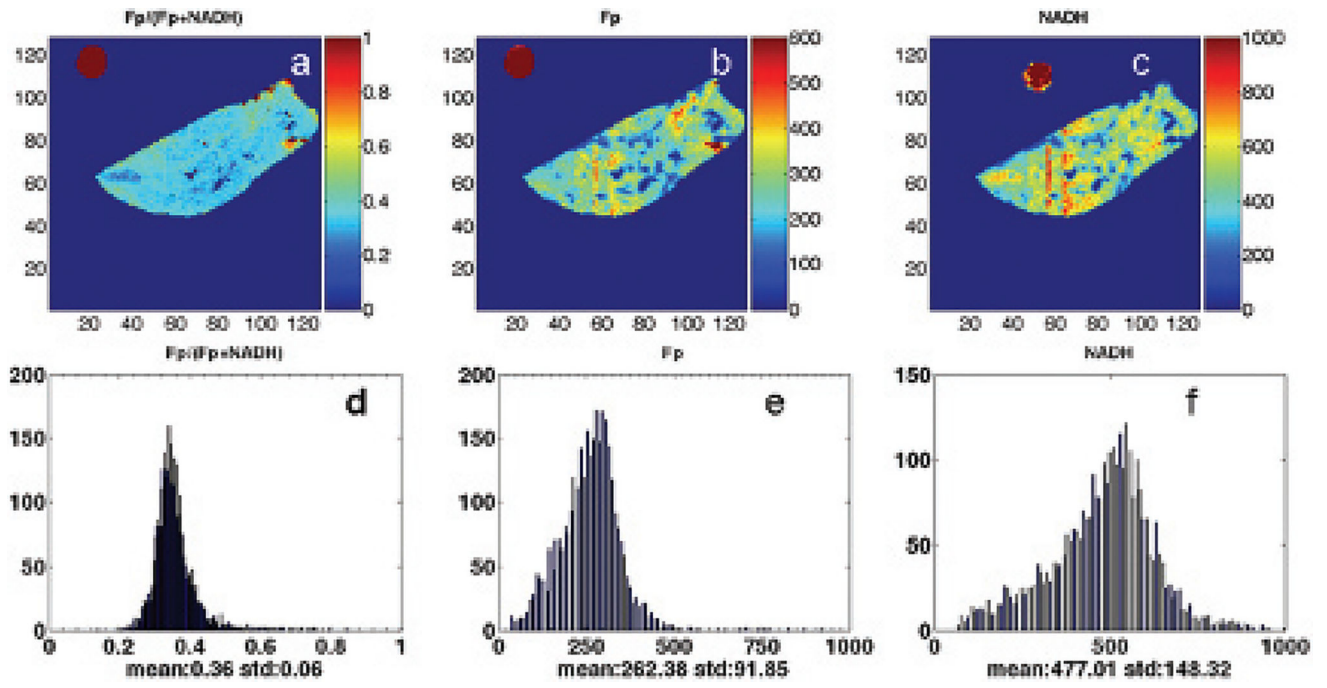


**Fig. 28.2.** Typical pseudo-color redox images (top row) and their corresponding histograms (bottom row) of the control group (coronal section, milling depth 0  $\mu\text{m}$ ). Image matrix:  $128 \times 128$ , resolution: 100  $\mu\text{m}$ .



Group ( $\bar{x}$ ) average values of Fp, NADH and Fp redox ratio and standard deviations (SD) for 3 pancreases in each group.

**Table 28.1**

	$\bar{x}$ Fp redox ratio	$\bar{x}$ SD of Fp ratio	$\bar{x}$ NADH	$\bar{x}$ SD of NADH	$\bar{x}$ Fp	$\bar{x}$ SD of Fp
Control	0.35±0.04	0.06±0.02	558±64	144±46	299±75	79±45
Pre-malignant	0.38±0.06	0.11±0.01	293±56	158±49	163±45	79±17
Unpaired t-test	0.49	0.02	0.01	0.73	0.07	0.98